Developmental Cell
Article

Probing Intrinsic Properties of a Robust Morphogen Gradient in *Drosophila*

Feng He,[1,3,6] Ying Wen,[1,6] Jingyuan Deng,[1,4] Xiaodong Lin,[5] Long Jason Lu,[1,4] Renjie Jiao,[3] and Jun Ma[1,2,*]
[1]Division of Biomedical Informatics
[2]Division of Developmental Biology
Cincinnati Children's Hospital Research Foundation, 3333 Burnet Avenue, Cincinnati, OH 45229, USA
[3]Institute of Biophysics, Chinese Academy of Sciences, 15 Datun Road, Beijing 100101, China
[4]Department of Biomedical Engineering
[5]Department of Mathematical Sciences
University of Cincinnati, Cincinnati, OH 45221, USA
[6]These authors contributed equally to this work
*Correspondence: jun.ma@cchmc.org
DOI 10.1016/j.devcel.2008.09.004

SUMMARY

A remarkable feature of development is its reproducibility, the ability to correct embryo-to-embryo variations and instruct precise patterning. In *Drosophila*, embryonic patterning along the anterior-posterior axis is controlled by the morphogen gradient Bicoid (Bcd). In this article, we describe quantitative studies of the native Bcd gradient and its target Hunchback (Hb). We show that the native Bcd gradient is highly reproducible and is itself scaled with embryo length. While a precise Bcd gradient is necessary for precise Hb expression, it still has positional errors greater than Hb expression. We describe analyses further probing mechanisms for Bcd gradient scaling and correction of its residual positional errors. Our results suggest a simple model of a robust Bcd gradient sufficient to achieve scaled and precise activation of its targets. The robustness of this gradient is conferred by its intrinsic properties of "self-correcting" the inevitable input variations to achieve a precise and reproducible output.

INTRODUCTION

Development is a reproducible and robust process that must correct not only variations intrinsic to the governing molecular events, but also embryo-to-embryo differences (Kerszberg and Wolpert, 2007; Lander, 2007; Arias and Hayward, 2006). In *Drosophila*, development along the anterior-posterior (A-P) axis is scaled with embryo length, effectively correcting embryo size variations (Holloway et al., 2006; Houchmandzadeh et al., 2002). The primary determinant specifying A-P patterning is the morphogenetic protein Bicoid (Bcd), which is distributed as a concentration gradient (Driever and Nüsslein-Volhard, 1988; Ephrussi and Johnston, 2004). It instructs development of the anterior structures by directly recognizing and activating its downstream targets (Burz et al., 1998; Driever and Nüsslein-Volhard, 1989; Ma et al., 1996; Struhl et al., 1989). One such target is Hunchback (Hb), which is expressed in the anterior half of the embryo and is responsible for thoracic development. While it is well established that Hb expression is precise and scaled with embryo length (Houchmandzadeh et al., 2002), how such precision and scaling is achieved remains controversial (Gibson, 2007; Holloway et al., 2002; Patel and Lall, 2002; Reinitz, 2007; Yucel and Small, 2006). At first glance, this might appear to be a rather simple problem: since Hb is a direct target of Bcd following a strict input-output relationship (Gregor et al., 2007a), Bcd gradient behaviors can readily provide explanations on how Hb precision and scaling is achieved. However, unlike the steep on/off Hb profile that is relatively easy to measure and quantify, accurately detecting and quantifying an exponential decay Bcd profile represents a considerable technical and theoretical challenge (Gregor et al., 2007a; Reinitz, 2007). Previous embryo staining studies revealed a significant embryo-to-embryo variability of the Bcd gradient (Houchmandzadeh et al., 2002; Spirov and Holloway, 2002), suggesting that precise Hb expression requires additional filtering mechanisms (Aegerter-Wilmsen et al., 2005; Bergmann et al., 2007; Houchmandzadeh et al., 2005; Howard and ten Wolde, 2005). In contrast, results of a recent live-imaging study with a GFP-Bcd hybrid protein suggests that the Bcd gradient is sufficiently precise to account for Hb precision (Gregor et al., 2007a; Gregor et al., 2007b).

Interpretation of the differences between the live-imaging data—derived from the GFP hybrid protein—and embryo staining data of the native Bcd protein remains the subject of intense interest and further study (Gregor et al., 2007a; Reinitz, 2007). This is not merely a technical or mathematic problem, but directly affects how we think about precision control mechanisms during development. In the study described here, we ask the following questions through quantitative analyses of the native Bcd protein and its target Hb: (1) Does the native Bcd gradient exhibit a similar embryo-to-embryo reproducibility as observed in the live-imaging study? (2) Is the Bcd gradient itself scaled with embryo length and how? (3) Does Bcd gradient precision contribute directly to Hb precision? (4) Is the positional information of a precise Bcd gradient sufficient to account for Hb precision? Our results show that, similar to the live-imaging analysis, the native Bcd gradient is highly reproducible and itself exhibits scaling properties. Increased Hb variability in mutant embryos (from *staufen* females) is directly associated with increased Bcd gradient variations, demonstrating that a precise Bcd gradient is

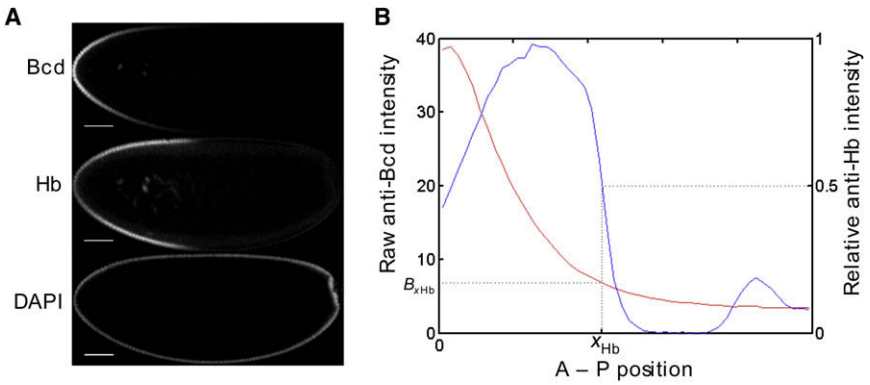

Figure 1. Experimental Approaches and Parameters

(A) Shown are digital images of a WT embryo (w^{1118}), at early nuclear cycle 14, detecting antibodies against Bcd (top), Hb (middle), or stained with DAPI (bottom). Scale bar, 50 μm.

(B) Shown are Bcd and Hb intensity profiles to illustrate the parameters used in our analysis (see text for additional parameters and further details).

necessary for Hb precision. Our results also show that a precise Bcd gradient in wild-type (WT) embryos still has positional errors that are larger than Hb boundary variability. We describe analyses aimed at uncovering mechanisms for both Bcd gradient scaling and correction of its residual positional errors. We present a simple Bcd gradient model with robust "self-correcting" properties sufficient for scaled and precise activation of its target genes.

RESULTS

Experimental Approach and Parameters for Analysis

We explored a modified staining procedure to detect Bcd intensities in WT embryos (see Experimental Procedures for details). For our analysis, we used anti-Bcd and anti-Hb antibodies to simultaneously detect Bcd and Hb proteins in individual embryos (Figure 1A). High-resolution digital images of double-stained embryos at early nuclear cycle 14 were captured, and Bcd and Hb intensities measured and plotted against the A-P position *x* (Figure 1B). Throughout this work, Bcd intensities were captured within a linear range and expressed as raw data (unless otherwise noted), without any normalization or adjustment at either imaging or data processing steps. To minimize measurement errors, all images for a group of embryos were captured with identical settings in a single imaging cycle. In addition, we "spiked" embryos with those lacking Bcd (from bcd^{E1} females) to specifically measure background intensities under identical experimental conditions. To facilitate our analysis, we measured the following values for each embryo: embryo length (*L*), the Hb expression boundary (x_{Hb}), which is the A-P position where Hb intensity is 50% maximal, the highest Bcd intensity (B_{max}), Bcd intensity at the anterior (B_0), and Bcd intensity at the Hb boundary position (B_{xHb}). When describing a group of embryos, any value given refers to the mean unless noted otherwise; for example, x_{Hb} of a group of embryos refers to the group's mean Hb expression boundary position.

Native Bcd Profiles Are Reproducible in WT Embryos

Figure 2A shows that Bcd intensity profiles in WT embryos are highly reproducible (see Figure 2B for Hb intensity profiles). This analysis represents the measurement of 28 double-stained WT embryos at early nuclear cycle 14. Bcd intensities were measured by scanning the nuclear layer of the dorsal part of individual embryos and plotted against normalized A-P position (fractional embryo length; *x*/*L*). The reproducibility of the Bcd profiles in these WT embryos is qualitatively evident. First, these profiles are visually less variable than those reported previously using stained WT embryos (Gregor et al., 2007a; Holloway et al., 2006; Houchmandzadeh et al., 2002; Spirov and Holloway, 2002). In addition, Bcd intensities from these embryos do not appear to have a higher variability than the data measured from individual nuclei of a single embryo (see Figure S1C available online), suggesting that Bcd intensity variations among individual embryos at early nuclear cycle 14 are comparable to those between neighboring nuclei in single embryos. As shown in Figures 2C and 2D, Bcd intensities of random pairs of WT embryos or random pairs between WT and 1 × −*bcd* embryos both exhibit a linear relationship, further supporting the suggestion that the measured Bcd profiles in WT embryos are reproducible and intensities are linear to the *bcd* gene dose (see also Gregor et al. [2007a]).

To quantify reproducibility of native Bcd profiles in WT embryos, we calculated the mean and standard deviation of Bcd intensities along the A-P position (see Figure S2 and Supplemental Discussion). We plotted Bcd intensity noise (SD/mean) as a function of *x*/*L*. The raw Bcd intensity noise (Figure 2E, red line) is ~10%–20% for almost the entire A-P length of the embryos. The noise of background-subtracted Bcd intensities (Figure 2E, blue line) remains low in the anterior half of the embryos (generally ~15%–20%). These results are in contrast with those of previously reported studies with stained embryos (Holloway et al., 2006; Houchmandzadeh et al., 2002; Spirov and Holloway, 2002), but are in agreement with a recently reported live-imaging study (Gregor et al., 2007a). As shown in Figure 2E, Bcd intensity noise (blue line) exhibits a gradual increase toward the posterior, but even in this part of the embryo it remains <60%, a noise level lower than that detected by the live-imaging approach (Gregor et al., 2007a). Bcd intensity variations among individual embryos and between neighboring nuclei of single embryos exhibit overall similar profiles (Figure S1D). Figure 2F shows the effect of correcting background and measurement noise on Bcd intensity variations (see Experimental Procedures for details).

Bcd Profiles Are Scaled with Embryo Length

The analysis described above indicates that Bcd intensity profiles in WT embryo as a function of normalized A-P position (*x*/*L*) are highly reproducible. It is well established that the Hb expression boundary x_{Hb} is scaled with embryo length (i.e., x_{Hb} is correlated with *L*; $r = 0.52$; $p = 0.005$; also see Houchmandzadeh

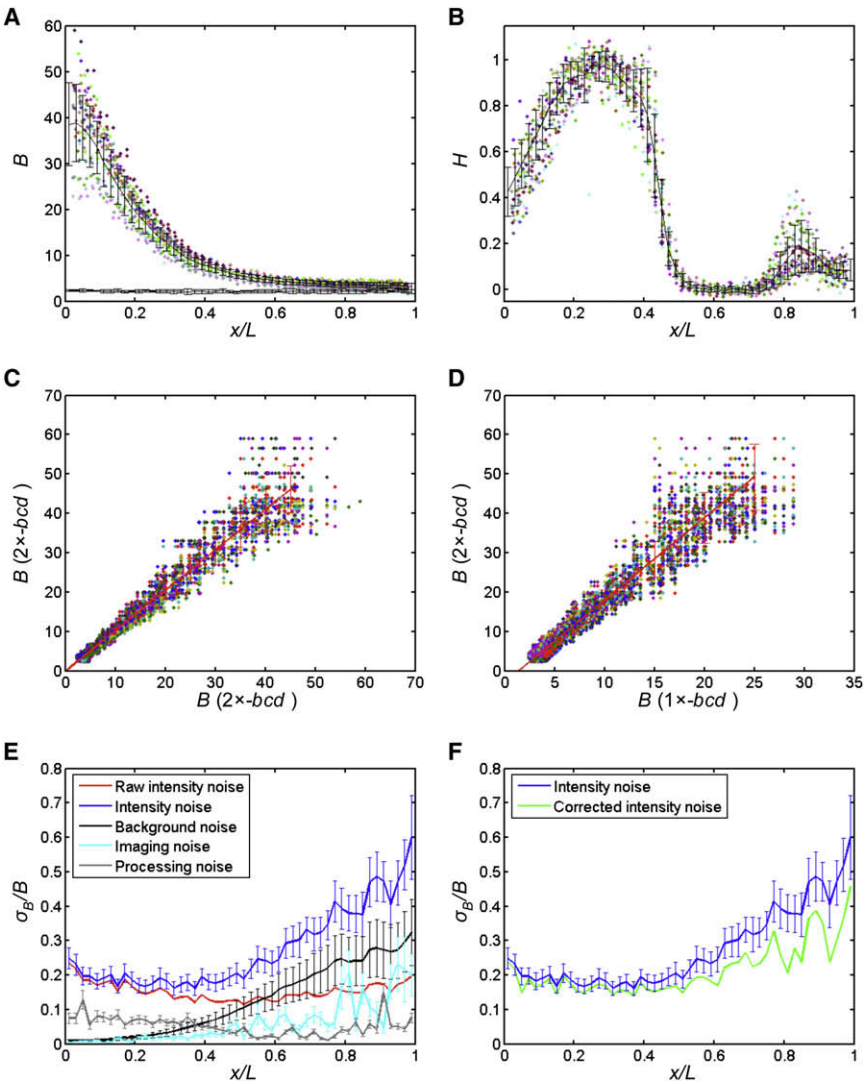

Figure 2. Bcd Profiles Are Reproducible in WT Embryos

(A) Shown are raw Bcd intensity profiles from 28 WT embryos at early nuclear cycle 14. Different colors represent different embryos. The mean intensities and error bars are shown. The line at the bottom represents the intensity profiles in embryos lacking Bcd; the background noise normalized by its own raw intensities (shown as the error bars) is 10%–20% throughout the entire A-P length of bcd^{E1} embryos.

(B) Shown are normalized Hb intensity profiles from the same WT embryos.

(C) Scatter plot of raw Bcd intensities between paired WT embryos. The data are from all possible pairs of 17 WT embryos (the red line, with error bars shown, represents a linear fit of $y = 1.01[x - 0.04]$; $r = 0.98$; $p < 10^{-20}$).

(D) Scatter plot of raw Bcd intensities between WT (2 × *-bcd*) and 1 × *-bcd* embryos. The data shown represent all pairs of 17 WT embryos and 10 1 × *−bcd* embryos (a linear fit for the data is $y = 1.98[x - 1.16]$; $r = 0.97$; $p < 10^{-20}$).

(E) Bcd intensity noise (SD/mean) for WT embryos. The red line shows raw Bcd intensity noise, while the blue line shows background-subtracted Bcd intensity noise (without any further adjustments). Error bars are from bootstrapping. Also shown in this figure are background noise (black line, normalized by Bcd intensities of WT embryos; see Equation [5]), imaging noise (cyan), and processing noise (gray). See Experimental Procedures for details.

(F) Shown are background-subtracted Bcd intensity noise profiles with (green) or without (blue) correcting for measurement and background noise. See Experimental Procedures for further details.

et al. [2002]). However, how embryo length variations may affect Bcd gradient precision in embryos has not been fully characterized (Gregor et al., 2007a). When discussing precision and scaling of the Bcd gradient, we pay particular attention to Bcd profile behaviors at and around x_{Hb}, because they will directly affect our interpretation of how precision and scaling of Hb expression is achieved. We reasoned that, if the Bcd gradient itself is scaled with embryo length, Bcd intensity variations as a function of normalized A-P position *x/L* should be lower than those measured as a function of absolute distance from the anterior (*x* in microns), particularly at and around x_{Hb}. In other words, scaling of the Bcd gradient is expected to "make" Bcd profiles in this region more precise when A-P position is normalized than without normalization. Our results shown in Figure 3A clearly demonstrate such a reduction in Bcd intensity variations at and around x_{Hb}, supporting the notion that the Bcd gradient is scaled with embryo length.

We conducted a second test to further analyze the effect of embryo length variations on Bcd gradient precision. In this test, we divided the WT embryos into two groups according to their embryo length and analyzed their average Bcd intensity profiles. However, before we discuss our Bcd data, we use the Hb expression boundary x_{Hb} that is known to be scaled with embryo length to help illustrate how our analysis works. As shown in Figure 3B, the two average Hb intensity profiles (for large and small embryos) are different from each other when plotted as a function of absolute distance from the anterior (*x* in microns), with small embryos as a group having a shorter x_{Hb} than large embryos ($p = 0.016$, Student's t test). However, when these two Hb intensity profiles are expressed as a function of *x/L* (Figure 3C), they converge and effectively eliminate x_{Hb} differences ($p = 0.42$). The observed convergence of the two average Hb intensity profiles is simply another way of illustrating the well-documented embryo length scaling of x_{Hb} in WT embryos. In a similar analysis for Bcd, the inset in Figure 3D shows that the average Bcd intensities for large and small embryos are significantly different from each other at and around x_{Hb} when plotted as a function of absolute A-P position *x* ($p = 0.01$ at x_{Hb}; see Figure 3 legend for p values at surrounding locations). However, when these two curves are plotted as a function of normalized A-P position *x/L*, they converge near x_{Hb} (Figure 3E, inset), effectively eliminating Bcd intensity differences ($p = 0.20$ at x_{Hb}; see

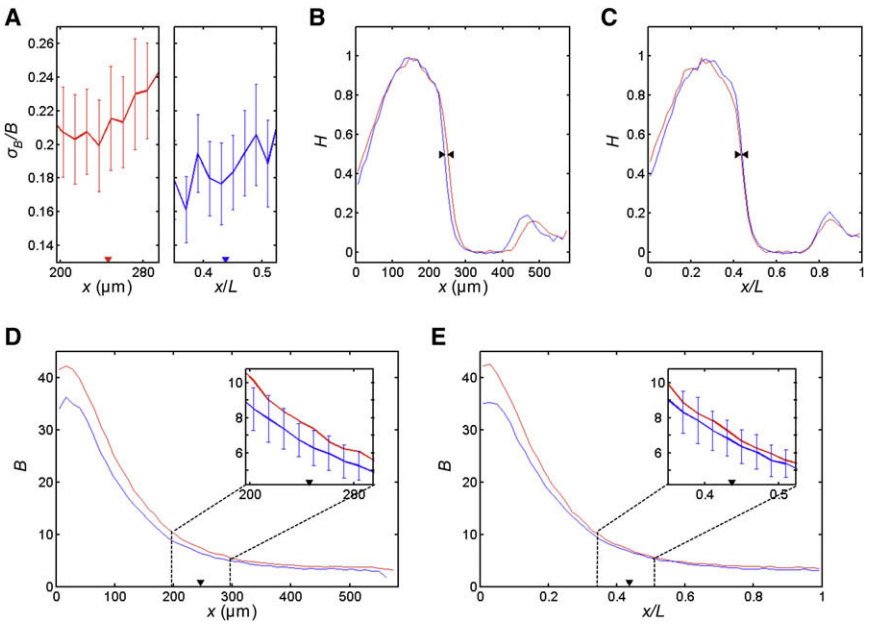

Figure 3. The Native Bcd Gradient Is Scaled with Embryo Length

(A) Shown are Bcd intensity variations around the x_{Hb} position when A-P position is measured as absolute distance from the anterior (left panel) or as fractional embryo length (right panel). Bcd intensities are background-subtracted with no further adjustments. The x_{Hb} position is marked with a solid arrowhead in each panel for reference.

(B and C) Shown are average Hb intensity profiles for large (red) and small (blue) WT embryos as a function of absolute distance from the anterior x (B) or fractional embryo length, x/L (C). In this analysis, the 28 WT embryos were divided into the top half (large) and bottom half (small) based on their simple L ranks. Note the separation of the two curves at x_{Hb} (pointed by arrowheads) in (B) and their convergence in (C).

(D and E) Shown are average raw Bcd intensity profiles for large (red) and small (blue) WT embryos as a function of x (D) or x/L (E). The x_{Hb} position is marked with solid arrowheads. The insets show the average curves (with error bars shown for one) in the region surrounding x_{Hb}. Student's t test was conducted to determine p values at x_{Hb} and its surrounding locations. Listed below are p values for seven intervals in the A-P order, with the value at the x_{Hb} position shown in italics: 0.032, 0.035, 0.008, *0.008*, 0.052, 0.034, and 0.015 for (D), and 0.18, 0.38, 0.12, *0.20*, 0.30, 0.50, 0.17 for (E).

Figure 3 legend for p values at surrounding locations). Together, these analyses demonstrate that the Bcd intensity profiles are scaled with embryo length to provide precise and scaled activator information for Hb activation in WT embryos.

Probing Mechanisms of Embryo Length Scaling of Bcd Gradient

Our analysis of Bcd intensity profiles of large and small embryos (Figures 3D and 3E) also provides critical insights into mechanisms of embryo length scaling. In particular, our results show that B_0 is significantly higher in large embryos as a group than in small embryos (p = 0.024, Student's t test). In order to investigate the propagation of this positive correlation along the A-P length, we plotted the correlation coefficient between B and L (r_{B-L}) as a function of either x or x/L. As shown in Figure 4A, r_{B-L} peaks at $x = \sim 200$ μm ($r_{B-L} = 0.66$; p = 10^{-4}; see inset for a scatter plot between B and L at this position) and then drops gradually toward the posterior as a function of x. In the x/L plot (Figure 4B), however, r_{B-L} begins to drop almost immediately from the anterior, effectively attenuating the propagation of this anteriorly originated positive correlation toward x_{Hb} and beyond (profiles of Spearman's rank correlation coefficient exhibit behaviors similar to those shown in Figures 4A and 4B [data not shown]). The inset in Figure 4B shows a scatter plot between B and L at the peak position, as identified from the x/L plot.

In order to test whether a positive B_0-L correlation might be sufficient to explain embryo length scaling of Bcd profiles, we performed simulation studies with the exponential decay Bcd profile $B = B_0 \exp(-x/\lambda)$, where λ is the length constant (Houchmandzadeh et al., 2002). Our simulation results demonstrate two features expected of scaling when B_0 is correlated with L; namely: (1) a reduced Bcd noise in x/L plot compared with that in x plot (Figure 4C); and (2) the convergence of the average Bcd intensity curves for large and small embryos in the middle of the embryo (data not shown). Both of these properties are absent when B_0 and L are uncorrelated (Figure 4D and data not shown), demonstrating that a B_0-L correlation is sufficient to explain our observed scaling properties of the Bcd gradient.

Reduced Bcd Reproducibility in *Stau* Embryos Directly Contributes to Hb Variations

To further understand the molecular mechanisms of developmental precision and size scaling, we analyzed *Drosophila* mutants that exhibit variable Hb expression patterns. The only *Drosophila* mutant that has been reported to affect Hb precision is the maternal gene *staufen* (*stau*; Crauk and Dostatni [2005]; Houchmandzadeh et al. [2002]). Hb boundary in embryos from homozygous $stau^{HL}$ females (referred to as *stau* embryos) is almost twice as variable as in WT embryos (σ = 1.43% and 2.78% embryo length for WT and *stau* embryos, respectively; see Figure 2B and the inset in Figure 5A for Hb intensity profiles in WT and *stau* embryos, respectively). Unlike in WT embryos, x_{Hb} and L are no longer correlated in *stau* embryos ($r = 0.043$; p = 0.83), suggesting a loss of Hb boundary scaling. In order to understand defects of *stau* embryos, we measured Bcd gradient intensities in these embryos (Figure 5A). To ensure a direct comparison, *stau* embryos were stained side by side with WT embryos and images taken in the same imaging cycle as WT embryos. Overall, Bcd intensities in these embryos exhibit a greater variability (Figure 5B, green line) than in WT embryos (blue line). Bcd intensity noise is over 20% in the anterior half of *stau* embryos and is increased dramatically toward the posterior. In addition, unlike in WT embryos, Bcd intensity variations in *stau* embryos are not lower around the x_{Hb} region when expressed as a normalized A-P position than without normalization

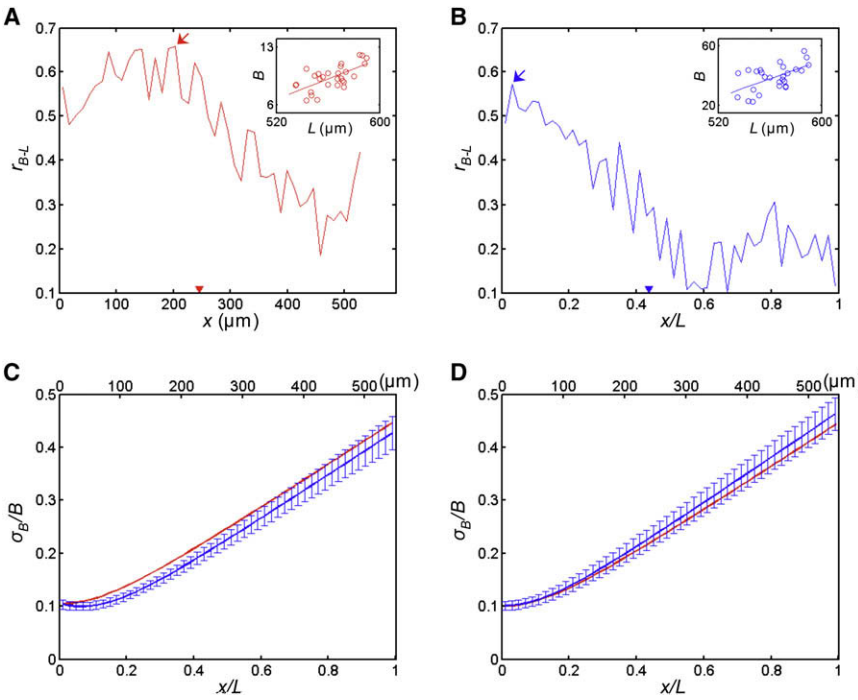

Figure 4. Scaling Mechanisms for the Bcd Gradient in WT Embryos

(A and B) Shown is correlation coefficient r_{B-L} between Bcd intensity and embryo length as a function of x (A) or x/L (B). The insets show scatter plot for B and L at their respective peak positions (r = 0.66, p = 10^{-4} for [A], inset; r = 0.57, p = 10^{-3} for [B], inset). For 1 × and 3 × *−bcd* embryos, peak r_{B-L} values are: 0.5 at 98 μm (p = 0.01) and 0.6 at 168 μm (p = 0.005), respectively. As in WT embryos, x_{Hb} exhibited a correlation with L in 1 × and 3 × *−bcd* embryos: r = 0.61 (p = 1.4 × 10^{-3}) and r = 0.66 (p = 10^{-4}), respectively.

(C and D) Simulated data showing Bcd intensity variations as a function of x (red, top scale) or x/L (blue, bottom scale). Simulations were performed with (C) or without (D) a B_0-L correlation (r = 1). We also performed simulation analyses by varying the B_0-L correlation coefficient, r. We found that at an r of 0.44, the Bcd intensity variation at x_{Hb} remains significantly lower when expressed as a function of normalized embryo length than without normalization (p < 0.05, Student's t test), indicating that this B_0-L correlation level is sufficient, in our simulations, to establish the Bcd scaling property shown in Figure 4C. See Experimental Procedures for further details.

(Figure 5B, inset), suggesting a loss of scaling of the Bcd gradient (see Figure S3 and Supplemental Discussion).

In order to directly determine whether increased Bcd variability is responsible for increased x_{Hb} variability in *stau* embryos, we grouped the embryos according to their normalized Hb boundary positions. We reasoned that, if Hb boundary variations in *stau* embryos are caused by Bcd intensity variations, embryos that have an anteriorly shifted x_{Hb} as a group should cross Bcd thresholds at a more anterior position than embryos with a posteriorly shifted x_{Hb}. Figures 5C and 5D show, respectively, the average Hb and Bcd intensity profiles of the two groups of *stau* embryos that have either an anteriorly or posteriorly shifted x_{Hb}. As shown in the inset in Figure 5D, the two average Bcd intensity curves cross thresholds at different A-P positions, with the anteriorly shifted group crossing at more anterior positions (see Figure 5 legend for p values). In a similar test for WT embryos (data not shown), the average Bcd intensity curve for embryos with a smaller (than mean) normalized x_{Hb}, as a group, does not cross thresholds at more anterior positions than the other group (see Figure 5 legend for p values). These results suggest that increased Bcd intensity variability in *stau* embryos directly contributes to increased x_{Hb} variations.

Positional Errors of the Bcd Gradient and Hb Precision

Our studies described thus far suggest that Bcd gradient precision is necessary for precise Hb expression. In order to determine whether the observed Bcd profile reproducibility is sufficient to account for Hb precision in WT embryos, we converted the measured Bcd intensity errors to positional errors, σ_x (i.e., errors in x at which individual Bcd profiles cross given thresholds [Gregor et al., 2007a]). Our results show that σ_x is ~3.5%–4% embryo length around x_{Hb}, which is more than twice the observed Hb boundary variations (1.4% embryo length; see Figure 6A for positional errors of Bcd and Hb). Even after Bcd intensity errors are corrected for measurement and background noise, positional errors remain higher for Bcd (~3%–3.5% embryo length) than for Hb (generally <2% embryo length). These results suggest that a precise Bcd gradient, although necessary, is insufficient on its own to account for Hb precision (also see Reinitz [2007]). We must stress here again that our Bcd intensities are not adjusted or normalized in any way except background subtraction (see also Supplemental Discussion). Previous models proposed to explain Hb precision—assuming that Bcd profiles are noisy—all suggest the operation of additional factors (Aegerter-Wilmsen et al., 2005; Bergmann et al., 2007; Houchmandzadeh et al., 2005; Howard and ten Wolde, 2005), but most of these efforts remain at a theoretical level, underscoring a need for experimental investigations.

In order to further understand mechanisms controlling Hb expression and precision, we focused our analysis on two parameters that directly describe Hb activation by Bcd in embryos. The first parameter is the Hill coefficient, n, which has a best fit of 5.1 ± 2.7 for WT embryos, a value that is in agreement with a recent estimate in embryos (Gregor et al., 2007a) and with our biochemical studies (Ma et al., 1996). The Hill coefficient depicts the steepness of the Hb boundary, but n variations have little or no effect on Hb boundary position. The second parameter is the Bcd level at the Hb boundary position B_{xHb}, which is the measured Bcd threshold for Hb activation in individual embryos. B_{xHb} has a variability of 24% (5.0 ± 1.2) in WT embryos, a variability higher than that of Bcd profiles. If our observed B_{xHb} variations represent meaningful differences that are indicative of the properties of embryos (as opposed to measurement errors), then such variations must be incorporated into our analysis of the Bcd-Hb relationship.

We entertained the possibility that B_{xHb} variations might actually be reflective of a correction mechanism(s) that further reduces positional errors of an already precise Bcd gradient.

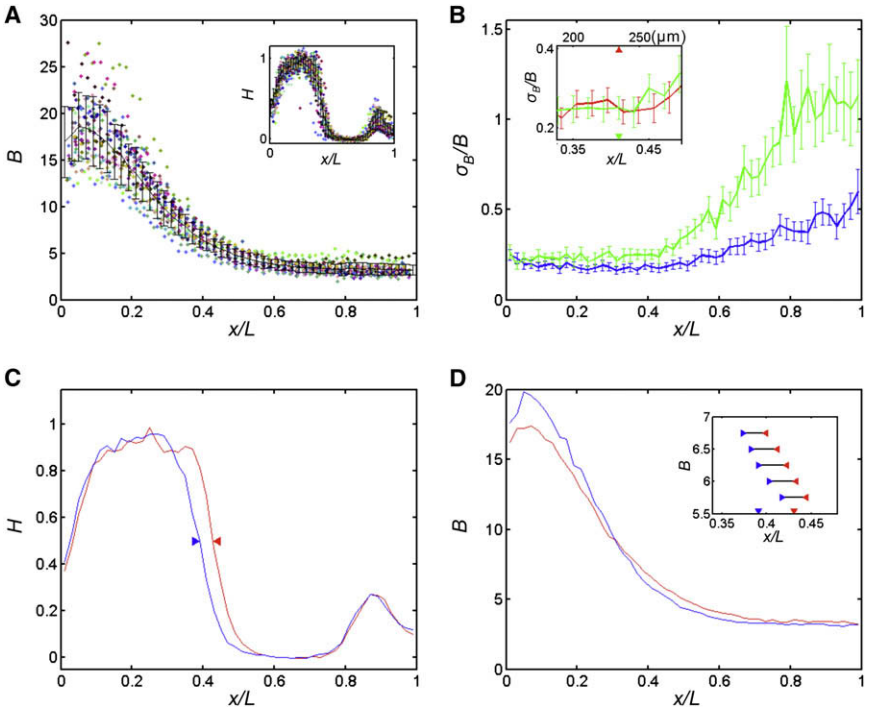

Figure 5. Increased Bcd Variability in *Stau* Embryos Directly Contributes to Hb Variations

(A) Shown are raw Bcd intensity profiles from 26 *stau* embryos (from $stau^{HL}$ females) at early nuclear cycle 14. Different colors represent different embryos. The mean intensities and error bars are shown. Inset shows normalized Hb intensity profiles from the same *stau* embryos.

(B) Bcd intensity noise in *stau* embryos (green) and, for comparison, in WT embryos (blue). Bcd intensities represent background-subtracted values with no further adjustments. Error bars are from bootstrapping. Inset shows the Bcd intensity noise profiles as a function of either *x* (red, top scale) or *x*/*L* (green, bottom scale) in regions surrounding x_{Hb} (x_{Hb} positions on both scales are marked with solid arrowheads).

(C and D) Average Hb (C) and Bcd (D) intensity profiles for *stau* embryos that have an anteriorly shifted (blue) or posteriorly shifted (red) normalized Hb boundary position (two groups represent bottom and top halves based on simple x_{Hb}/L ranks, respectively). (D) Inset shows that the normalized A-P positions at which the two average Bcd intensity curves cross given thresholds are different (student's t test p value for the five indicated thresholds–from high to low–are: 0.052, 0.063, 0.031, 0.063, and 0.054; a similar test for WT embryos reveals the following p values: 0.26, 0.28, 0.22, 0.12, and 0.12). For reference, the average x_{Hb} positions for the two groups of *stau* embryos are marked with solid arrowheads in the inset in (D).

Our analysis reveled a positive correlation between B_{xHb} and the length constant, λ ($r = 0.44$; $p = 0.018$; see Figure 6B for a scatter plot of B_{xHb} and λ), a correlation that is further improved for embryos at a more uniform developmental stage ($r = 0.57$; $p = 0.014$; Spearman's rank correlation coefficient, $r_S = 0.49$; $p = 0.038$; see Experimental Procedures for details on developmental stage definitions). In order to determine whether the observed B_{xHb}-λ correlation could reduce positional errors of the Bcd gradient, we conducted simulation studies with the exponential decay Bcd profile, $B = B_0 \exp(-x/\lambda)$, and the Hill equation for Hb expression, $H = B^n / (B^n + B_{xHb}{}^n)$. All parameters in our simulations were based on experimentally determined values, resulting in a mean x_{Hb}/L of 0.44 under all simulation conditions (see Experimental Procedures for details). In the absence of any correlations, normalized x_{Hb} variability, σ_x, was 6.1% embryo length (Figure 6C), which was reduced to 1.1% embryo length when both B_0-*L* and B_{xHb}-λ correlations were applied (Figure 6D). Simulations with either B_0-*L* or B_{xHb}-λ correlation alone (Figures 6E and 6F) resulted in an x_{Hb} variability of 5.4% and 2.3% embryo length, respectively. Furthermore, unlike in Figure 6D, where Hb expression is both precise and scaled (i.e., x_{Hb} is correlated with *L*; $r = 0.93$), Hb expression is not scaled with embryo length in Figure 6F (i.e., x_{Hb} is uncorrelated with *L*; $r = -0.006$). These simulation results show that a scaled and precise Hb boundary requires both B_0-*L* and B_{xHb}-λ correlations. Further simulation studies of altering the parameters *L* and B_{xHb} revealed that a Bcd gradient, based on the two observed properties, is robust. In particular, target gene precision is insensitive to embryo length variations (Figure 6G) or movements of the target boundary position (Figure 6H), features in full agreement with experimental data (Crauk and Dostatni, 2005; Houchmandzadeh et al., 2002).

DISCUSSION

In a developing embryo, cells need to make unambiguous decisions in choosing their own fates by expressing distinct sets of genes (Levine and Davidson, 2005; Arias and Hayward, 2006). Such decisions must be reproducible from embryo to embryo, despite individual and environmental differences (Kerszberg and Wolpert, 2007; Lander, 2007; Patel and Lall, 2002). In *Drosophila*, cells adopting the anterior fate express Hb, a direct target of the Bcd morphogen gradient (Burz et al., 1998; Driever and Nüsslein-Volhard, 1989; Ma et al., 1996; Struhl et al., 1989). Despite embryo size variations, Hb expression boundary is precise and scaled with embryo length (Holloway et al., 2006; Houchmandzadeh et al., 2002). How Hb precision is achieved directly affects our understanding of developmental scaling and reproducibility. Although a recent live-imaging study provided unprecedented new insights into both the dynamics and precision of the Bcd gradient (Gregor et al., 2007a, 2007b), it had to rely on a GFP-Bcd hybrid protein. In this article, we describe quantitative studies to analyze the behaviors of the native Bcd gradient and its target Hb. Our results show that: (1) the native Bcd gradient is precise and scaled with embryo length; (2) a precise Bcd gradient is necessary for Hb precision; and (3) a precise Bcd gradient still has positional errors that are greater than Hb boundary variations. Our results uncover correlated "self-correcting" input

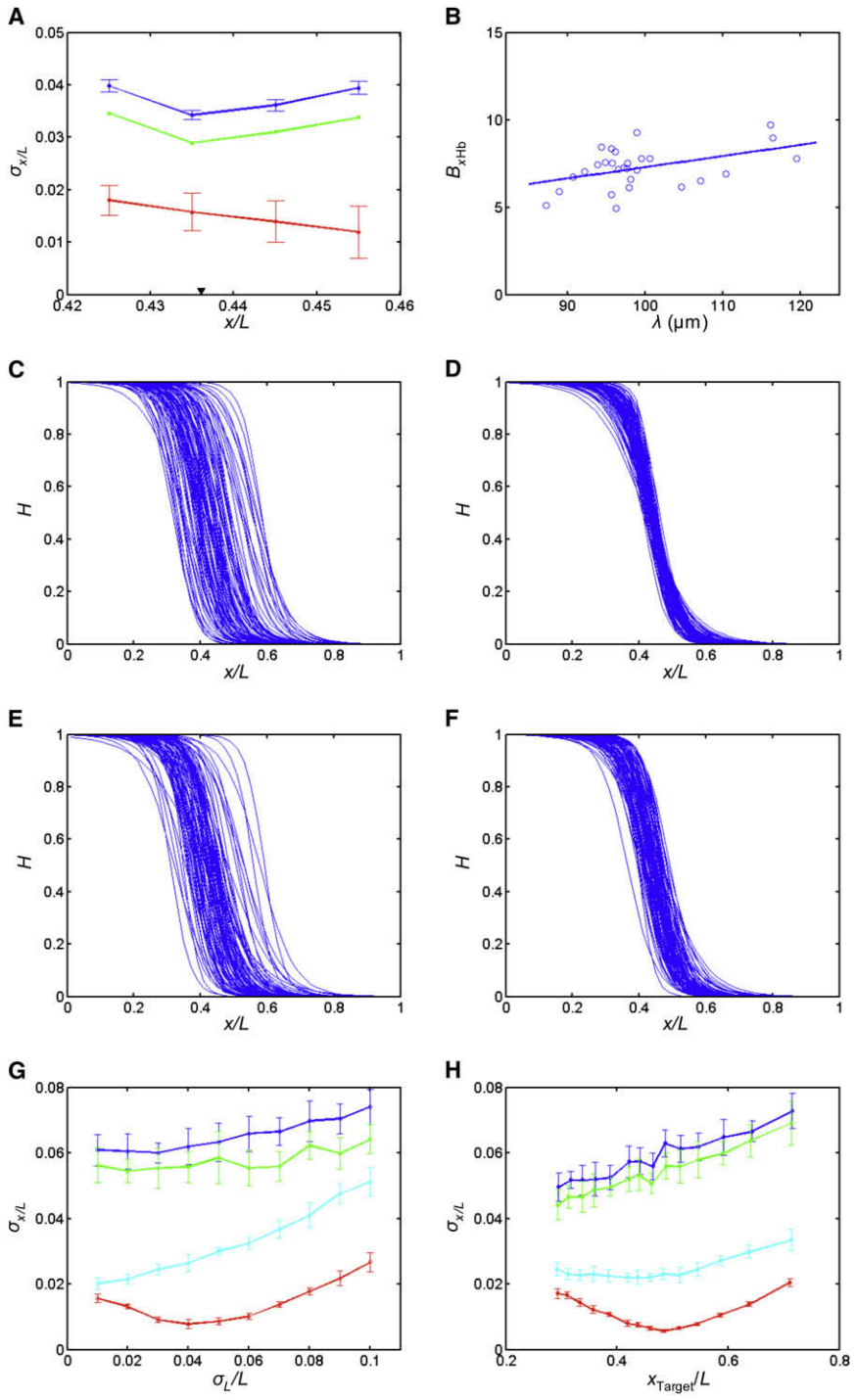

Figure 6. Correction of Positional Errors of the Bcd Gradient

(A) Positional errors ($\sigma_{x/L}$) of the Bcd gradient in WT embryos converted from its intensity errors with (green) or without (blue) the correction for measurement and background noise. Also shown are positional errors of the Hb expression profiles (red). The conversion of intensity errors to positional errors was performed as previously described (Gregor et al., 2007a).

(B) Shown is a scatter plot for B_{xHb} and λ in WT embryos.

(C–F) Simulated Hb expression profiles obtained under the following simulation conditions: no correlations (C), both B_0-L and B_{xHb}-λ correlations (D; $r = 1$), B_0-L correlation alone (E; $r = 1$), and B_{xHb}-λ correlation alone (F; $r = 1$). The mean Hb boundary position x_{Hb}/L is 0.44 for all panels, with a variation σ_x of 6.1%, 1.1%, 5.4%, and 2.3% embryo length for(C)–(F), respectively.

(G) A Bcd gradient model sufficient to correct embryo length variations. Shown are SDs of normalized Hb boundary ($\sigma_{x/L}$) as a function of embryo length variations (σ_L/L). The data are from simulated results that were conducted under the following conditions: both B_0-L and B_{xHb}-λ correlations (red), no correlations (blue), B_0-L correlation alone (green), and B_{xHb}-λ correlation alone (cyan). See Experimental Procedures for details.

(H) A robust Bcd gradient sufficient for precise and scaled target gene activation at different A-P positions. In these simulations, Bcd thresholds were varied to change the boundary positions (x_{Target}) of hypothetical target genes of Bcd. Shown are SDs of normalized target boundary $\sigma_{x/L}$ as a function of normalized x_{Target}. Color code is the same as in (G). Note that the simulated x_{Target} under the condition of B_{xHb}-λ correlation alone (cyan) is not scaled with embryo length (see text for further details).

variations as the underpinnings of a robust gradient system sufficient for scaled and precise target gene activation.

Bcd Gradient Precision and Scaling

A major finding of our current studies is that native Bcd profiles are not only reproducible, but also scaled with embryo length. Unlike previous embryo staining studies, we: (1) use raw Bcd intensity data captured within a linear range; (2) specifically measure background intensities under identical experimental conditions; and (3) avoid any normalization or adjustment of Bcd intensity data (except background subtraction when necessary). These and other improvements have enabled us to accurately measure Bcd profiles in stained embryos (see Supplemental Discussion). Our studies reveal Bcd properties expected of scaling. In particular, Bcd intensities are more precise when measured as a function of normalized A-P position than without such normalization (Figure 3A). Moreover, Bcd intensity in the anterior (B_0) is correlated with L. This correlation drops rapidly as a function of x/L, effectively preventing its propagation toward normalized x_{Hb} and beyond (Figure 4B). We show that a B_0-L correlation is sufficient to account for the observed scaling properties of Bcd gradient in WT embryos (Figures 4C and 4D). We currently do not know exactly the source(s) of our observed B_0-L correlation. If the amount of *bcd* mRNA deposited into an egg during oogenesis is proportional to the egg volume, it could represent a source for our observed B_0-L

correlation. This simple model of Bcd gradient scaling contrasts with an alternative model (Gregor et al., 2007b), in which Bcd gradient precision is maintained throughout the A-P length by "counting" the nuclear number, rather than measuring distance. A fundamental difference between these two models reflects how Bcd intensity variations near the anterior are interpreted: while our model suggests that such variability is biologically meaningful and responsible for size scaling through the observed B_0-L correlation, the alternative model interprets it as a mere consequence of the difference in the locations (but not L-correlated amounts/rates) of Bcd protein synthesis.

Hb Precision Requires a Precise Bcd Gradient

Our analysis of *stau* embryos demonstrates that a precise Bcd gradient is necessary for precise Hb expression. Bcd profiles in *stau* embryos are more variable than in WT embryos (Figure 5B), most likely resulting from the increased variations in *bcd* mRNA localization and/or amount (Crauk and Dostatni, 2005). Concurrently, Hb expression is more variable in *stau* embryos and exhibits properties indicative of a loss of scaling. More importantly, normalized x_{Hb} position in *stau* embryos is positively correlated with Bcd level at the mean normalized x_{Hb} ($r = 0.52$, $p = 0.006$ for *stau* embryos; $r = -0.34$, $p = 0.078$ for WT embryos), a correlation that is further improved for embryos at a more uniform developmental stage ($r = 0.80$, $p = 0.016$ for *stau* embryos; $r = 0.17$, $p = 0.50$ for WT embryos; Spearman's rank $r_S = 0.83$, $p = 0.010$ for *stau* embryos; $r_S = 0.29$, $p = 0.25$ for WT embryos). These results, together with those shown in Figure 5, suggest that increased Hb variability in *stau* embryos is a direct consequence of increased Bcd gradient variations. Our observed Bcd gradient behaviors in *stau* embryos are different from those described in a previous report (Houchmandzadeh et al., 2002), and we attribute these and other differences to methods in detecting and analyzing Bcd intensities (see Supplemental Discussion). On a technical note, we suggest—based on the following two observations—that stained embryos are suitable for studying developmental precision when data are captured and analyzed properly (also see Wu et al. [2007b]). First, Bcd intensities detected in our stained WT embryos have variations comparable to live-imaging data (Gregor et al., 2007a). In addition, Bcd intensity variability for a group of stained WT embryos is comparable to that for neighboring nuclei of single embryos (Figure S1D).

Positional Errors of Bcd Gradient and Hb Boundary Precision

As demonstrated by our studies and suggested by Reinitz (Reinitz, 2007), positional information of a precise Bcd gradient is still more variable than the observed Hb precision. At the Hb boundary position, the Bcd gradient has already become very shallow and, thus, any Bcd intensity variations, even for a very precise gradient, would correspond to significant positional errors that reflect its intrinsic properties. In our study, the two parameters that directly describe the relationship between Bcd and Hb (n and Bcd threshold for Hb activation $B_{x\mathrm{Hb}}$) both exhibit variations. These variations could either reflect the true nature of the Bcd-Hb system, or may result merely from measurement uncertainties. We favor the former possibility (but we cannot formally exclude the latter), because our experimental results reveal a correlation between $B_{x\mathrm{Hb}}$ and λ capable of correcting the observed positional errors of the Bcd gradient. We currently do not know exactly the source(s) of this observed correlation. However, there have been examples of coupling between an activator's stability and its ability to activate transcription (Lipford et al., 2005; Muratani et al., 2005; von der Lehr et al., 2003; Wu et al., 2007a; see also Tanaka [1996]). In addition or alternatively, it is sensible to imagine that stochastic, embryo-to-embryo variations in chromatin structure may affect both Bcd diffusion and its effective DNA binding affinity. Regardless of the details that remain to be uncovered, both possibilities support a link between Bcd gradient formation and activation in embryos, a notion consistent with the idea that nuclei are important for both degradation and diffusion properties of Bcd (Gregor et al., 2007b).

A Simple Model of a Robust Bcd Gradient

The studies described here suggest that the sources of Hb scaling and precision can be directly traced to the behaviors of the native Bcd gradient. We identify two intrinsic properties of Bcd relevant to developmental precision: (1) formation of a precise and scaled Bcd gradient resulting from a correlation between B_0 and L; and (2) correction of its own positional errors through a link between gradient formation and activation (i.e., $B_{x\mathrm{Hb}}$-λ correlation). Our simulation studies show that a Bcd gradient with these two observed properties is sufficient to achieve a precise and scaled Hb boundary without theoretically provoking the involvement of any additional factors (Figure 6D). Consistent with experimental observations (Crauk and Dostatni, 2005; Houchmandzadeh et al., 2002), the Bcd gradient model based on these properties is robust: it is insensitive to embryo length variations (Figure 6G), and its precise action is applicable to targets with distinct boundary positions (Figure 6H). The robustness of this Bcd gradient model stems from mechanisms that self-correct the system's inevitable input variations arising from embryo-to-embryo differences. In particular, while egg size (L) variations are corrected by Bcd amount (B_0) to achieve scaling, variations in gradient formation (λ) are corrected by target recognition/activation ($B_{x\mathrm{Hb}}$) to enhance precision. According to our simple model, other factors, such as gap gene products, may affect the mean position of the Hb boundary (Houchmandzadeh et al., 2002; Perkins et al., 2006; Reinitz, 2007; Rivera-Pomar and Jackle, 1996; Simpson-Brose et al., 1994), but they are not required for Hb precision and scaling, a notion fully consistent with experimental data (Houchmandzadeh et al., 2002). Furthermore, since the two observed properties (correlations) are sufficient for the Bcd gradient to achieve a precise and scaled output, as shown by simulation studies (Figures 6C–6G), foreign activators (such as the yeast activator Gal4) expressed as A-P gradients in *Drosophila* embryos are expected to activate their targets in a precise and scaled manner if they possess these same properties (Crauk and Dostatni, 2005). It is relevant to note that the yeast activator Gal4 does possess a property that couples its degradation to its activation function (Muratani et al., 2005), and, furthermore, its effective affinity for target DNA sites in vivo is regulated by its activation potency (Tanaka, 1996). Finally, it has been shown that the nuclear concentration of Bcd has already become stable prior to nuclear cycle 14 (Gregor et al., 2007b), and, therefore, the robust properties of the Bcd gradient should be applicable throughout the entire relevant period of development.

The observations of a highly reproducible Bcd gradient have recently led to the suggestion that the system may be so precise that it approaches the limits set by basic physical principles (Gregor et al., 2007a; see also Tostevin et al. [2007]). Our results show that, while the Bcd gradient is highly reproducible, the system still faces input variations arising from embryo-to-embryo differences. A hallmark feature of biological systems is, to their advantage, the interconnections among the operating components and processes. Our studies suggest a robust Bcd gradient system that can self-correct its own inevitable input noise to achieve a precise and reproducible output. Our work thus underscores the importance of input variations, because their self-correcting properties are actually responsible for conferring the robustness to the system. Our simple model provides a new framework for developmental scaling and precision, and understanding its molecular and dynamic details represents future challenges.

EXPERIMENTAL PROCEDURES

Embryo Staining and Imaging

All embryos used in this study were collected at 25°C. Embryos were fixed and stained with antibodies, as described previously (Kosman et al., 1998), except for an extra fixation and permeability treatment (Patel et al., 2001) prior to antibody staining, procedures that likely have contributed to our observed reproducibility of Bcd profiles in WT embryos. Primary antibodies (rabbit anti-Bcd and guinea pig anti-Hb) were generous gifts of Paul Macdonald (Macdonald, 1990) and John Reinitz (Kosman et al., 1998), respectively. Secondary antibodies were Alexa-594-conjugated goat anti-rabbit and Alexa-488-conjugated goat anti-guinea pig antibodies (Molecular Probes). Nuclei were counterstained with DAPI (Sigma). Stained embryos were mounted in DABCO antifade (Sigma) on slides with or without bridges for midsagittal or flattened-embryo images, respectively. High-resolution digital images (1388 × 1040, 8 bits/pixel) were captured on Zeiss Imager Z1 ApoTome microscope with a Zeiss Plan Aprochromat objective through the use of Axiovision 4.5 software in linear setting without normalizations. Linearity throughout the entire A-P length of the embryo was experimentally confirmed with images with varying exposure time (data not shown). In addition, Bcd intensities captured on ApoTome and confocal microscopes exhibit a linear relationship (Figure S1A), indicating that data generated from both microscopes are directly comparable. In our study, a single imaging cycle refers to a period of operation during which all microscopic and imaging accessories, including computer and software, were kept on in an uninterrupted and continuous manner. For midsagittal images, embryos were first adjusted manually, when necessary, to obtain optimal dorsal-ventral orientation and A-P alignment (i.e., no tilt) under bright-field or DAPI channels. We estimate our focal plane selection has an uncertainty of the size of a nucleus (6–12 μm, depending on stage). We analyzed 13 images of individual embryos captured at 1 μm intervals along *z* and found the noise in *L* measurement, σ_L/L, caused by focal plane selection to be negligible (0.0004, 0.0006, and 3×10^{-16} for three different embryos) compared with our observed *L* variations in WT and *stau* embryos (0.028 and 0.045, respectively).

Intensity Measurements

All data presented in this study are from embryos at early nuclear cycle 14. These embryos have ~70–80 identifiable nuclei at the midsagittal plane on the dorsal side, and we selected embryos, the nuclei of which have just begun to elongate (nuclear height:width ratio in the range of ~1.3–1.7:1) and the posterior Hb expression level of which is <0.5. We also used a more stringent criterion of posterior Hb expression level (<0.25) for embryos at a more uniform developmental stage with similar results. In this study, we processed images automatically, where Bcd (or Hb) intensities were extracted by sliding a circular window the size of 61 pixels (<nuclear size) within the nuclear layer along the edges of the embryo (Houchmandzadeh et al., 2002). The scanning intervals along the A-P axis projection were either 18 pixels (~12 μm) or 2% embryo length to generate intensity data in the scale of *x* or *x*/*L*, respectively, for each embryo. We also extracted raw Bcd intensities by manually identifying the nuclear centers based on DAPI staining. As shown in Figure S1B, raw Bcd intensities captured automatically or manually exhibit a linear relationship, indicating that both sets of data are directly comparable. For flattened-embryo images, DAPI staining was used for nuclear identification in an automated way, where local background was subtracted and noise reduced by median filtering, followed by optimizations to set upper and lower thresholds for nuclear identification. Each embryo had ~1000–1500 nuclei identified. Raw Bcd intensities were extracted from the identified nuclei without adjustments, and data in the range of 10%–60% along the dorsal-ventral axis of embryos were used for analysis.

Background Measurement and Noise Correction

For our experiments, we directly measured background Bcd intensities; we used embryos lacking Bcd (from bcd^{E1} females) to "spike" those to be analyzed to ensure background measurement under identical experimental conditions. We note that each WT embryo has its own individual background level even when they were stained in the same batch. In our study, we used the mean of Bcd intensities from bcd^{E1} embryos for background subtraction. An alternative of utilizing Bcd intensities in the posterior of embryos for "individualized" background subtraction would require a problematic assumption that there are no Bcd molecules in the posterior (see Supplemental Discussion). We also conducted experiments to estimate two sources of measurement errors: imaging noise and data processing noise. For imaging noise, we captured images sequentially for individual embryos under identical settings and calculated the variance of intensity data across five images. For processing noise, we shifted intensity scanning centers by one pixel toward eight two-dimensional directions and calculated the variance across nine sets of data. For noise correction, we use a reported model (Houchmandzadeh et al., 2005; Wu et al., 2007b) to describe intensity measurement (with an upper hat denoting a random variable):

$$\widehat{I}_j = \widehat{\alpha} \times \widehat{n}_j + \widehat{\beta}, \tag{1}$$

where $\widehat{I}_j$ is measurement of background-subtracted fluorescence intensity, *j* corresponds to the position of the measurement on the embryo, $\widehat{\alpha}$ is the experimental rescaling factor, $\widehat{n}_j$ is the number of Bcd molecules at position *j*, and $\widehat{\beta}$ is the background noise. We denote imaging noise as $\widehat{\alpha}_1$ and processing noise as $\widehat{\alpha}_2$. We assume that these noises are independent and follow normal distributions. Thus, $\widehat{\beta}$, $\widehat{\alpha}_1$, and $\widehat{\alpha}_2$ can be written as $\delta_\beta \widehat{N}(0,1)$, $\delta_1 \widehat{N}(0,1)$, and $\delta_2 \widehat{N}(0,1)$, respectively, and intensity measurement $\widehat{I}_j$ can be written as:

$$\widehat{I}_j = m \times (1 + \widehat{\alpha}_1 + \widehat{\alpha}_2) \times \widehat{n}_j + \widehat{\beta}. \tag{2}$$

We define $\langle \widehat{I} \rangle = E(\widehat{I})$ and normalized variance $\eta^2(I) = \mathrm{var}(I)/\langle I \rangle^2$. When we measure $\widehat{\alpha}_1$, we assume the other variables have no contribution to the measurement. We denote $\widehat{I}_{\alpha_1}$ as $m \times (1 + \widehat{\alpha}_1) \times \langle \widehat{n}_j \rangle$; thus $\delta_1^2 = \mathrm{var}(\widehat{\alpha}_1) = \eta^2(\widehat{I}_{\alpha_1})$. Similarly, $\delta_2^2 = \eta^2(\widehat{I}_{\alpha_2})$. Thus, the normalized variance of $\widehat{I}_j$ can be written as:

$$\eta^2(\widehat{I}_j) = \eta^2(\widehat{n}_j) \times (1 + \eta^2(\widehat{I}_{\alpha_1}) + \eta^2(\widehat{I}_{\alpha_2})) + \eta^2(\widehat{I}_{\alpha_1}) + \eta^2(\widehat{I}_{\alpha_2}) + \frac{\delta_\beta^2}{\langle \widehat{I}_j \rangle^2}, \tag{3}$$

$$\eta^2(\widehat{n}_j) = \frac{\eta^2(\widehat{I}_j) - \eta^2(\widehat{I}_{\alpha_1}) - \eta^2(\widehat{I}_{\alpha_2}) - \frac{\delta_\beta^2}{\langle \widehat{I}_j \rangle^2}}{1 + \eta^2(\widehat{I}_{\alpha_1}) + \eta^2(\widehat{I}_{\alpha_2})}, \tag{4}$$

and, since $\eta^2(\widehat{I}_{\alpha_1}) \approx 0.01$, $\eta^2(\widehat{I}_{\alpha_2}) \approx 0.01$,

$$\eta^2(\widehat{n}_j) = \eta^2(\widehat{I}_j) - \eta^2(\widehat{I}_{\alpha_1}) - \eta^2(\widehat{I}_{\alpha_2}) - \frac{\delta_\beta^2}{\langle \widehat{I}_j \rangle^2}. \tag{5}$$

Parameter Calculation and Simulations

All parameter estimations and simulations were done on Matlab software (MathWorks). The λ and *n* values for individual embryos were calculated as follows. Background-subtracted Bcd intensity values were first fitted with $B = a \exp(-x/\lambda)$ by excluding the data at 0%–10% embryo length, because Bcd profiles in this part of the embryo do not follow the exponential decay function (Houchmandzadeh et al., 2002, 2005). A linear fit of ln*B* to *x* in the range of 10%–50% embryo length was then used to estimate *a* and λ, where *a* is an extrapolated value that could be understood as the hypothetical B_0 if Bcd profiles

followed the exponential decay function throughout the entire A-P length. Hb expression obeys the Hill equation, $H = B^n/(B^n + B_{xHb}{}^n)$, where B_{xHb} is the experimentally determined Bcd intensity value at x_{Hb}. The n value was estimated by a least-square nonlinear fit in the range of 30%–50% embryo length, a region that corresponds to the Hb expression switch. All parameters used in simulations were based on experimentally observed values with minor adjustments: $L = 550 \pm 15$ μm; $\lambda = 100 \pm 8$ μm; $n = 5 \pm 1$; $B_0 = 50 \pm 5$ cu (arbitrary concentration units); and $B_{xHb} = 4.5 \pm 1$ cu. For Figures 6G and 6H, simulations were carried out with L and B_{xHb} being set as variables as indicated. Each simulation was performed with an n of 100 and error bars were from 10 independent simulations.

SUPPLEMENTAL DATA

Supplemental Data include Supplemental Discussion and three supplemental figures and can be found with this article online at http://www.developmentalcell.com/supplemental/S1534-5807(08)00377-8.

ACKNOWLEDGMENTS

We thank Paul Macdonald and John Reinitz for anti-Bcd and anti-Hb antibodies, Gary Struhl and the Christiane Nusslein-Volhard laboratory for fly stocks, Rhonda VanDyke, Mi-Ok Kim, and members of the Ma laboratory for discussions, and David Cheung for images used in estimating embryo length measurement noise. This work was supported in part by grants from NIH and NSF (to J.M.), and NSFC (to J.M. and R.J.). R.J. acknowledges support from NSFC (30623005) and 973 program (2005CB522804).

Received: May 26, 2008
Revised: August 19, 2008
Accepted: September 8, 2008
Published: October 13, 2008

REFERENCES

Aegerter-Wilmsen, T., Aegerter, C.M., and Bisseling, T. (2005). Model for the robust establishment of precise proportions in the early Drosophila embryo. J. Theor. Biol. *234*, 13–19.

Bergmann, S., Sandler, O., Sberro, H., Shnider, S., Schejter, E., Shilo, B.Z., and Barkai, N. (2007). Pre-steady-state decoding of the Bicoid morphogen gradient. PLoS Biol. *5*, e46.

Burz, D.S., Pivera-Pomar, R., Jackle, H., and Hanes, S.D. (1998). Cooperative DNA-binding by Bicoid provides a mechanism for threshold-dependent gene activation in the *Drosophila* embryo. EMBO J. *17*, 5998–6009.

Crauk, O., and Dostatni, N. (2005). Bicoid determines sharp and precise target gene expression in the *Drosophila* embryo. Curr. Biol. *15*, 1888–1898.

Driever, W., and Nüsslein-Volhard, C. (1988). A gradient of bicoid protein in *Drosophila* embryos. Cell *54*, 83–93.

Driever, W., and Nüsslein-Volhard, C. (1989). Bicoid protein is a positive regulator of hunchback transcription in the early *Drosophila* embryo. Nature *337*, 138–143.

Ephrussi, A., and Johnston, D.S. (2004). Seeing is believing. The bicoid morphogen gradient matures. Cell *116*, 143–152.

Gibson, M.C. (2007). Bicoid by the numbers: quantifying a morphogen gradient. Cell *130*, 14–16.

Gregor, T., Tank, D.W., Wieschaus, E.F., and Bialek, W. (2007a). Probing the limits to positional information. Cell *130*, 153–164.

Gregor, T., Wieschaus, E.F., McGregor, A.P., Bialek, W., and Tank, D.W. (2007b). Stability and nuclear dynamics of the bicoid morphogen gradient. Cell *130*, 141–152.

Holloway, D.M., Reinitz, J., Spirov, A., and Vanario-Alonso, C.E. (2002). Sharp borders from fuzzy gradients. Trends Genet. *18*, 385–387.

Holloway, D.M., Harrison, L.G., Kosman, D., Vanario-Alonso, C.E., and Spirov, A.V. (2006). Analysis of pattern precision shows that *Drosophila* segmentation develops substantial independence from gradients of maternal gene products. Dev. Dyn. *235*, 2949–2960.

Houchmandzadeh, B., Wieschaus, E., and Leibler, S. (2002). Establishment of developmental precision and proportions in the early *Drosophila* embryo. Nature *415*, 798–802.

Houchmandzadeh, B., Wieschaus, E., and Leibler, S. (2005). Precision domain specification in the developing *Drosophila* embryo. Phys. Rev. E Stat. Nonlin. Soft. Matter Phys. *72*, 061920.

Howard, M., and ten Wolde, P.R. (2005). Finding the center reliably: robust patterns of developmental gene expression. Phys. Rev. Lett. *95*, 208103.

Kerszberg, M., and Wolpert, L. (2007). Specifying positional information in the embryo: looking beyond morphogens. Cell *130*, 205–209.

Kosman, D., Small, S., and Reinitz, J. (1998). Rapid preparation of a panel of polyclonal antibodies to *Drosophila* segmentation proteins. Dev. Genes Evol. *208*, 290–294.

Lander, A.D. (2007). Morpheus unbound: reimagining the morphogen gradient. Cell *128*, 245–256.

Levine, M., and Davidson, E.H. (2005). Gene regulatory networks for development. Proc. Natl. Acad. Sci. USA *102*, 4936–4942.

Lipford, J.R., Smith, G.T., Chi, Y., and Deshaies, R.J. (2005). A putative stimulatory role for activator turnover in gene expression. Nature *438*, 113–116.

Ma, X., Yuan, D., Diepold, K., Scarborough, T., and Ma, J. (1996). The *Drosophila* morphogenetic protein Bicoid binds DNA cooperatively. Development *122*, 1195–1206.

Macdonald, P.M. (1990). Bicoid mRNA localization signal: phylogenetic conservation of function and RNA secondary structure. Development *110*, 161–171.

Arias, A.M., and Hayward, P. (2006). Filtering transcriptional noise during development: concepts and mechanisms. Nat. Rev. Genet. *7*, 34–44.

Muratani, M., Kung, C., Shokat, K.M., and Tansey, W.P. (2005). The F box protein Dsg1/Mdm30 is a transcriptional coactivator that stimulates Gal4 turnover and cotranscriptional mRNA processing. Cell *120*, 887–899.

Patel, N.H., Hayward, D.C., Lall, S., Pirkl, N.R., DiPietro, D., and Ball, E.E. (2001). Grasshopper hunchback expression reveals conserved and novel aspects of axis formation and segmentation. Development *128*, 3459–3472.

Patel, N.H., and Lall, S. (2002). Precision patterning. Nature *415*, 748–749.

Perkins, T.J., Jaeger, J., Reinitz, J., and Glass, L. (2006). Reverse engineering the gap gene network of *Drosophila* melanogaster. PLoS Comput. biol. *2*, e51.

Reinitz, J. (2007). Developmental biology: a ten per cent solution. Nature *448*, 420–421.

Rivera-Pomar, R., and Jackle, H. (1996). From gradients to stripes in *Drosophila* embryogenesis: filling in the gaps. Trends Genet. *12*, 478–483.

Simpson-Brose, M., Treisman, J., and Desplan, C. (1994). Synergy between the Hunchback and Bicoid morphogens is required for anterior patterning in *Drosophila*. Cell *78*, 855–865.

Spirov, A.V., and Holloway, D.M. (2002). Making the body plan: precision in the genetic hierarchy of *Drosophila* embryo segmentation. In Silico Biol. *3*, 89–100.

Struhl, G., Struhl, K., and Macdonald, P. (1989). The gradient morphogen bicoid is a concentration-dependent transcriptional activator. Cell *57*, 1259–1273.

Tanaka, M. (1996). Modulation of promoter occupancy by cooperative DNA binding and activation-domain function is a major determinant of transcriptional regulation by activators in vivo. Proc. Natl. Acad. Sci. USA *93*, 4311–4315.

Tostevin, F., ten Wolde, P.R., and Howard, M. (2007). Fundamental limits to position determination by concentration gradients. PLoS Comput. Biol. *3*, e78.

von der Lehr, N., Johansson, S., Wu, S., Bahram, F., Castell, A., Cetinkaya, C., Hydbring, P., Weidung, I., Nakayama, K., Nakayama, K.I., et al. (2003). The F-box protein Skp2 participates in c-Myc proteosomal degradation and acts as a cofactor for c-Myc-regulated transcription. Mol. Cell *11*, 1189–1200.

Wu, R.C., Feng, Q., Lonard, D.M., and O'Malley, B.W. (2007a). SRC-3 coactivator functional lifetime is regulated by a phospho-dependent ubiquitin time clock. Cell *129*, 1125–1140.

Wu, Y.F., Myasnikova, E., and Reinitz, J. (2007b). Master equation simulation analysis of immunostained Bicoid morphogen gradient. BMC Syst. Biol. *1*, 52.

Yucel, G., and Small, S. (2006). Morphogens: precise outputs from a variable gradient. Curr. Biol. *16*, R29–R31.